The climate role of CO_2 – nature's telling from 400 Mio. years

Thomas Anderl (bhu.research@gmx.net)
BHU Research

Research Article

Keywords: paleoclimate, climate modelling, CO2 temperature relationship

Posted Date: May 14th, 2021

DOI: https://doi.org/10.21203/rs.3.rs-524780/v1

Abstract

The broader public demand reproducibility of scientific results particularly related to hot societal topics such as climate change. Our studies focus on the 80:20-rule to identify the essentials from the readily observable. It is found that the paleo-records on the past 400 Mio. years well constrain the compound universal climate role of CO_2, this being represented by a very simple formula in line with previous sophisticated simulation results.

1. Introduction

Earth presently receives on average 240 W/m^2 of insolation (planetary albedo taken into account) [1]. In equilibrium, Earth radiates the same amount back to space, corresponding to -18°C in the blackbody approximation. The actual surface temperature is far higher with an average of about + 15°C. Therefore, something must be delivering heat to the surface in addition to insolation. When looking for the sources, a hint comes from a well-known experience: clear-sky nights exhibit relatively low Earth surface temperatures while cloudy nights remain relatively warm. Thus, the atmosphere is contributing to the heat variability at the surface, with water molecules as the dominant components.

However during the current geologic eon, the water content in the atmosphere is a passive reactant to otherwise driven temperatures, acting as an amplifier. When looking for the temperature driving processes, key candidates are the insolation (in particular the varying solar activity and modulation by the planetary albedo), tectonic movements (e.g. with their impact on ocean and wind currents), large volcanic activities, forms of life, extra-terrestrial events (bolide impacts, cosmic rays), and atmospheric composition beyond water content. Apparently through history, all these components have played their role in driving Earth's near-surface atmospheric temperature.

Regarding the atmospheric composition, CO_2 is recognized as a temperature driving agent. A clear sign comes from the well-known transmission spectrum of infrared radiation from Earth's surface into space: It reveals strong absorption by atmospheric CO_2 which to all existing knowledge, is contributing to the atmospheric heat. Thus, the wide-spread scepticism about the climate-determining role of CO_2 cannot be directed towards its existence per se, rather towards its extent.

The present analysis is devoted to the search for the empirically obvious related to the climate role of CO_2, including its relation to the further driving forces. Starting point are the paleo-reconstructions on surface temperature and atmospheric CO_2 concentration, with focus on the period 50 – 35 Mio. years before present (Ma BP) [2, 3], 400 ka BP (Vostok ice core data [4]), and the entire past 400 Ma BP [5,6]. These measurement data are found to be well reproduced by a simple model concentrating on the climate driving forces, basically identified as modulated insolation and CO_2. From this observation-based approach, the CO_2 contribution to equilibrium climate is judged universally well constrained in its compound effect, i.e. with all related effects taken into account, and is clearly disentangled from the opposite causation, the CO_2 concentration following temperature variabilities.

2. Puzzling The Climate Contribution Of Co2

2.1. Eocene, 50 – 35 Ma BP

First let us think of designing an experiment to measure the impact of the atmospheric CO_2 concentration onto the surface-air temperature. The CO_2 concentration needed to be changed and for each change, its value and the corresponding temperature recorded. Other temperature influences needed to be neglectable or well controlled. It turns out that Earth has performed such an experiment in the past. During the Eocene, in the period 35–50 Ma BP, atmospheric CO_2 has steadily been removed by sequestration while recording its concentration and the corresponding temperature via proxies. Other temperature influences are judged negligible. This assumption is considered a first-order approximation subjected to potential amendment as the time horizon and the data base widen in the course of the further analysis. The span of the CO_2 concentration has been from 1600 to 500 ppmv in the considered period, the temperature span from about 28 to 20°C.

An interpretation of the 'measurement' data (i.e. the proxy reconstructions) has previously been presented [2, 3]. In the present studies, these reconstruction data are found to follow a simple relationship between the CO_2 concentration (hereafter pCO_2 in the unit ppmv) and the entailed temperature (T_{CO2}), in the further course referred to as the Eocene (CO_2-temperature) relationship:

$$T_{CO2} = \ln(pCO_2/22) * 6.68°C. \quad (1)$$

From the historical CO_2 concentrations of [3] (here used in course representation), the related temperatures are determined according to the preceding Eocene relationship. A slight correction is applied to account for the steady solar luminosity increase with time (ΔT_{sol}) by approximating [5] via

$$\Delta T_{sol} = -0.01514 * t\,°C, \quad (2)$$

with t the time from present into the past in million years, and by applying 0.75 °C/(W/m^2) for the radiative forcing-to-temperature sensitivity (see e.g. [3]).

In Figure 1, the resulting $T = T_{CO2} + \Delta T_{sol}$ (smooth blue line) is compared with the 'measured' data given in [2] (orange wiggly line). The simple logarithmic function (equation 1) for the temperature impact from the atmospheric CO_2 concentration is well able to reproduce the temperatures of the considered period 50-35 Ma BP and beyond, extending to 60 Ma BP. As a sensitivity test, the two coefficients in T_{CO2} (equation 1) are changed by ±1 % and the resulting temperature boundaries depicted in Figure 1 by the dotted bright-blue lines.

Conclusion from the Eocene: As the primary change process, the atmospheric CO_2 concentration was steadily reduced in the period of 50 to 35 Ma BP. Roughly, a difference of 1100 ppmv in the CO_2 concentration is followed by a temperature difference of 8°C. This causal relationship is well explained by

simulation programs [2, 3]. At the same time, the simple 2-parameter logarithmic function of Eq. (1), the Eocene relationship, is able to reflect the compound effect of all underlying processes.

2.2. Late Quaternary, 420 ka BP until present

To explore the general applicability of the simple Eocene relationship, it is examined for a period with heavy disturbances to the pure CO_2 influence: the Late Quaternary with its dominant waxing and waning ice sheets, in cause alternating the surface albedo and thus, the absorbed surface insolation. The present study is based on the Vostok ice core data [4]. The herein reported CO_2 concentrations are used to derive the CO_2-effected temperature contributions according to the Eocene relationship (T_{CO2}). The albedo effect ($\Delta T_{ice\text{-}Quaternary}$) is approximated with help of the also reported proxy-determined temperature variabilities (ΔT_{Vostok}) of [4] by adapting the linear δ^{18}O-sea level-albedo relationship of [3] via:

$$\Delta T_{ice-Quaternary} = (0.2 * \Delta T_{Vostok} - 2.5)\ °C. \quad (3)$$

The factor 0.2 has the meaning of α_T/α_p where α_p the polar amplification (in this work taken as 2) and α_T the proportionality factor for the global mean surface temperature, hence 0.4.

In Fig. 2, the resulting temperatures $T = T_{CO2} + \Delta T_{ice-Quaternary}$ are compared with the proxy-measured temperatures. The computed temperatures T (orange solid curve) are in good accordance with the measured temperatures (long-dashed dark blue from [4] and short-dashed bright blue from [2]).

The two contributions to the computed temperature T, originating from CO_2 and predominantly ice albedo, are depicted in Fig. 3. Each, CO_2 and ice albedo, influence the surface temperature at similar size. In a more general (and correct) view, $\Delta T_{ice-Quaternary}$ represents all terms not covered by T_{CO2}. From Fig. 2, it is inferred that the aggregate non-CO_2 temperature contribution largely follows a linear relationship to the global mean surface temperature.

Conclusion from the Late Quaternary, part 1: By switching on ice albedo as a massive second temperature determinant in addition to CO_2, the observed temperatures are also well reproduced with help of the Eocene CO_2-temperature relationship. The Eocene relationship is indicated as independent of other temperature-driving forces.

This raises the question about the CO_2-temperature relationship in the other direction: It is well known that temperature is viably directing the atmospheric CO_2 concentration. On the sceptics' side, there is remarkable supposition that the CO_2 concentration is predominantly driven by temperature, rather than by human emissions during the industrial age. For an examination, let us think of an experiment to measure the CO_2 concentration entailed by different temperatures. Again, nature has done such an experiment: in the Late Quaternary. By increasing and reducing ice coverage, albedo is being varied, by this the absorbed surface insolation and in turn, the surface temperature. Temperature and CO_2 concentration have been recorded via proxies educed from ice cores (see before), and the associated time via the ice core depth.

During the Late Quaternary, temperature is considered the predominant CO_2 change agent, other CO_2-determining processes judged disregardable.

Looking at the Vostok ice core data [4], the local temperature has varied by about 10°C between glacial and inter-glacial maxima, and the CO_2 concentration by 100 ppmv. 10°C temperature difference in the Vostok ice core data roughly relate to 5°C in the global average temperatures (see factor of 0.5 in Fig. 2). Thus, a change of 1°C of the global annual mean temperature is followed by a change of 20 ppmv in CO_2 concentration. This is a factor of 2 higher then resulting from theoretical research [7], where the CO_2 concentration (pCO_2) varies per 1°C of temperature change according to $pCO_2/27$ (ppmv). For pre-industrial pCO_2, this roughly results in 10 ppmv CO_2 concentration change caused by a 1°C temperature change.

Application of this theorical relationship to the temperature variabilities in the Vostok ice core data results in the CO_2 concentrations as depicted by the dashed orange and dotted gray lines of Fig. 4, for Vostok temperatures times 0.5 and raw Vostok temperatures, respectively; the solid blue line shows the CO_2 concentrations as reported from the ice cores.

Conclusion from the Late Quaternary, part 2: Nature reveals different CO_2-temperature relationships for either direction: (a) temperature driving CO_2, (b) CO_2 driving temperature. In direction (a), the atmospheric CO_2 concentration follows temperature changes by 10–20 ppmv per 1°C temperature change. In direction (b), a change of 10 ppmv in CO_2 concentration causes a temperature change of about 0.07°C. Regarding for instance a CO_2 concentration increase of 100 ppmv, the Eocene relationship indicates an induced temperature increase of 0.7°C. Since this temperature increase, in turn, causes a concentration change of 7–14 ppmv, about 7–14 % of the 100 ppmv-increase is to be attributed to the entailed temperature increase.

2.3. PETM, 56 Ma BP, and Devonian to Triassic, 400 – 200 Ma BP

So far, the Eocene CO_2-temperature relationship has proven applicable for two geological ages, the Eocene and the Late Quaternary. The next sections shall turn to other eons with yet different conditions. The first is the time of the Paleocene-Eocene Thermal Maximum (PETM), circa 56 Ma BP. In a previous computer simulation study [8], temperature and CO_2 conditions have been analyzed by varying the CO_2 concentration up to 9 times pre-industrial levels. In Fig. 5, the results of the simulation study (blue dots connected by the solid line) are compared with the Eocene relationship results, corrected by ΔT_{sol} (Eq. 2) for 56 Ma (orange dots connected by the dashed line); the black circle depicts the PETM condition according to [8].

Conclusion from the PETM-study: The simple Eocene CO_2-temperature relationship is well able to reflect the comprehensive understanding of nature as implemented in simulation programs.

In a further earlier study [9], the period of 400 to 200 Ma BP has been analyzed. Based on observed CO_2 concentrations [5], the related radiative forcings have been determined. In Fig. 6, these forcings (solid blue line) are compared to those given by the Eocene relationship (dashed orange line) by applying a sensitivity of 1.2°C/(W/m^2).

Conclusion from the 400 – 200 Ma-period: The pattern of the radiative forcing from earlier computer studies is well reproduced by the simple Eocene relationship. It is noted that a sensitivity of 1.2°C/(W/m^2) is required for the agreement, whereas 0.75°C/(W/m^2) are perceived as a generally applicable standard. At this point, no interpretation can be given on the sensitivity specifics of this case; as hypothesis, the difference may predominantly be attributed to water vapor.

2.4. Late Paleozoic, 420 Ma BP until present

So far, the considerations have each focused on rather specific periods. In the various periods, the Eocene CO_2-temperature relationship has proven as a viable tool to quantify the CO_2-induced temperature variabilities. In this paragraph, the entire Late Paleozoic from 400 Ma BP to present will be analyzed utilizing the Eocene relationship. The CO_2 data are now taken from [5] (as in the previous 400 – 200 Ma study, context of Fig. 6), and the temperature data from [6]. Either data are judged coherent state-of-the-art reconstructions for the considered period. Both data are shown together in Fig. 7, the blue (mostly upper) line for the temperature and the orange line for the CO_2 concentration.

From visual impression, the extremes exhibit rather consistent patterns: nearly the same CO_2 concentrations correspond to the respective temperatures at the minima and maxima (except at the maxima of 90 and 55 Ma BP). In between, CO_2 may lead temperature by circa 20 Ma (400 – 320 Ma BP) or lag by 20 Ma (280 – 220 Ma BP). From this, it is expected improbable to extract a statistically significant correlation between the two variables – if not artificially adapted for the 20 Ma-time shifts. Since there is no explanation in sight for a potential time lead / lag of this order, such statistical analysis is disregarded.

Instead, the Eocene relationship is applied to the CO_2 concentrations. The resulting temperatures are depicted in Fig. 8 (dashed orange line) with a constant subtraction of 3°C, and compared to the reconstructed (measured) temperatures (solid blue line). Besides the artificial 3°C-offset, the agreement between the two curves is perceived remarkably good. One may infer that the Eocene relationship represents the major temperature driving force.

However, it is known that the absorbed insolation is subject to modulations with time. Significant variability is to be expected from the constantly increasing solar luminosity (see $\Delta Tsol$ of Eq. 2), from surface albedo via snow and ice coverage (e.g. regarding the Late Paleozoic icehouse at around 300 Ma), and proposedly from the cyclic cosmic ray intensities [10]. Further significant temperature influence is expected from tectonic changes (the entire considered period covered by supercontinent Pangea assembly to break-up).

The cosmic ray intensity $\varphi(t)/\varphi(0)$ is taken from [10] and its temperature influence approximated via fit by

$$\Delta T_{crf} = -4 * \varphi(t)/\varphi(0)\ ^\circ\mathrm{C}. \quad (4)$$

The resulting variability of ~ 3 °C is found in consistency with [10].
The tectonic changes are apparent in the paleogeographic evolvement; Fig. 9 shows a course reconstruction of [11]. The temperature impact is approximated via multiplying the coverages (in percent) of landmass, mountains, and ice sheets by -0.2°C/%, and the coverages of water (shallow waters and deep ocean) by + 0.2°C/%, and applying a constant offset of -7°C:

$$\Delta T_{tec} = (\Sigma_i\ f_i * C_i - 7)\ ^\circ\mathrm{C}, \quad (5)$$

with i indicating the tectonic types, f_i the coverage-temperature impact described before, and C_i the respective coverages (Figure 9).

This approach means for instance: In case, land gives 1 % to water, then 0.2°C is contributed by the reduction of land coverage and another 0.2°C by the simultaneous increase of the water area, in total 0.4°C. Originally introduced to explore the tectonic influences, ΔT_{tec} in its given form is interpreted as predominantly reflecting albedo variabilities and in addition, overall land/water-driven climate variabilities (shift in the coverage ratio of continental vs. warm-humid climates).

To put this into perspective, a 1 % land increase from today's tectonics – with ocean and land coverages 0.71 and 0.29, respectively, the ocean and land solar surface absorptions of [1], and a sensitivity of 0.75°C/(W/m^2) – results in a temperature reduction of 0.26°C. More qualitatively, the albedo of water clouds is about 10 % higher over land than over oceans, 0.46 versus 0.42 [12], contributing to higher surface insolation at oceans than at land. In conclusion, the albedo interpretation of ΔT_{tec} and the chosen parameter set are viewed as principally supported by separate studies. For further instance, in the Late Paleozoic icehouse at around 300 Ma BP, the ice sheet contribution to ΔT_{tec} is -2.9°C if the ice area is recruited from water areas.

In summary, the total temperature is determined by

$$T = T_{CO2} + \Delta T_{sol} + \Delta T_{crf} + \Delta T_{tec}. \quad (6)$$

The result is depicted in Fig. 10 by the dashed orange line and compared to the reconstructed (measured) temperatures (solid blue line). The agreement is perceived fair, particularly regarding the extensive period of about 400 Ma covering a large variety of disparate conditions. The pattern of the agreement remains principally unchanged (not shown) if considering the 68 % confidence boundaries for the CO_2 concentrations of [5], the temperature discussion of [6], and a potential sensitivity dependency on the climate state by varying the non-CO_2-terms in Eq. (6) by ±□. The agreement of the present high-level consideration with observations is seen as confirmation that the major temperature-determining

components have been identified and that their respective contributions can be quantified by simple approximations.

By nature of the approximations, the regarded contributions subsume all relevant underlying processes. This particularly applies to the Eocene CO_2-temperature relationship comprising e.g. atmospheric water vapor variations with temperature, changing ocean-atmosphere interaction with varying atmospheric CO_2 concentration and temperature, and the temperature influence on the CO_2 concentration (see above, Late Quaternary). T_{CO2} in Eq. (6) gives the near-surface temperature if CO_2 was the only forcing. The further components of Eq. (6) act as correction terms, each again subsuming all underlying processes. These are explicitly incorporated in ΔT_{sol} (Eq. 2) by applying the sensitivity of 0.75°C/(W/m^2) and implicitly incorporated via the factors − 4 and f_i in ΔT_{crf} (Eq. 4) and ΔT_{tec}, (Eq. 5), respectively. Dependency of the sensitivity on the climate state is approximated as zero, cross-terms and higher-order terms in the forcing-to-temperature relationship are interpreted to be partly contained as averages in the insolation components of Eq. (6) (i.e. ΔT_{sol}, ΔT_{crf}, ΔT_{tec}) and to be partly attributed to the residuals.

To examine model alternatives, variations have been applied to Eq. (6). (A) First, the contribution from the cosmic ray flux is set to zero. With the parameters of ΔT_{tec} changing from − 0.2 to -0.3°C/%, from + 0.2 to + 0.3°C/%, and the constant to -15°C, the temperatures are given as depicted by the dotted gray line in Fig. 10. (B) From here, ΔT_{tec} is replaced by two components. (i) Snow/ice albedo is approximated by a linear relationship to temperature: for $T_{CO2} + \Delta T_{sol} > 17$°C, the relative albedo contribution is + 3°C; for lower temperatures, the contribution is $(T_{CO2} + \Delta T_{sol} - 11.5) \bullet 0.545$°C. (ii) A temperature contribution is introduced proportional to the ocean continental coverage [13], which is a measure for the eustatic sea level; this temperature contribution is taken proportional as 0.2°C per 1 % continental coverage difference with a constant offset of -6°C. This temperature contribution is interpreted to originate from albedo variabilities. The resulting temperatures are shown in Fig. 10 by the dot-dashed green line. (C) Introduction of effects from atmospheric oxygen variabilities leads to temperatures within the ranges exhibited in Fig. 10 (therefore not shown).

In general, the pursued selective and simple driving-force consideration cannot cater for the entirety of all related processes. Major contributions to the temperature variabilities are expected from strong volcanic activities (beyond the CO_2 effects) as well as from wind and ocean currents. The latter may be the cause for the deviations between about 50 and 30 Ma BP in Fig. 10 which decrease by circa − 4°C during this period (differences between solid blue and dashed orange lines in Fig. 10). Such progressive cooling may well be ascribed to changes in the ocean currents [14]. Also the model-to-reconstruction deviations before and after the center of the late Paleozoic icehouse (at about 300 Ma BP) are proposed to be predominantly attributed to warming contributions from – tectonically determined – ocean current specifics, these being largely reduced in the presence of wide-spread glaciation (i.e. at the center of the icehouse).

The proxy reconstructions used for the Late Paleozoic in this paragraph exhibit deviations from those used for the derivation of the Eocene relationship in § 2.1. Nevertheless, the original relationship of Eq. (1) reveals as best fit through the Late Paleozoic-analysis.

From comparison of Fig. 10 (dashed orange line) with Fig. 8, the summed effect of insolation variabilities (particularly from solar luminosity (ΔT_{sol}) and albedo) roughly acts as a constant temperature reduction of 3°C. As example for detailed insight, the single temperature contributions to T (Eq. (6), dashed orange line in Fig. 10) are depicted in Fig. 11.

For an illustration of reconstruction uncertainty effects, the 68 %-$p\mathrm{CO}_2$ confidence envelope is used for T_{CO2} of the dotted gray line in Fig. 10 and the results depicted by the dotted gray lines of Fig. 12. The relative temperature uncertainties are emulated as 0.3 times the relative $p\mathrm{CO}_2$ uncertainties (68% confidence). By this, the uncertainty increase with depth into the past is accounted for; the absolute height (factor 0.3) has intuitive character. It is interpreted that detailed error treatment cannot substantially alter the preceding considerations.

Conclusion: The attempt is perceived successful to describe the fundamental climate determinants by simple means. The Eocene CO_2-temperature relationship is revealed to be applicable throughout (at least) the past 400 Ma, as resulting from comparisons with paleo-reconstructions (Eocene, Late Quaternary, Late Paleozoic) together with plausibility considerations on the further major climate determinants. CO_2 delivers the major contribution to the climate variabilities. The second major influence stems from the modulation of the absorbed insolation by the sun's luminosity, the planetary albedo (via paleogeography/tectonics, or snow/ice and sea level), and potentially cosmic rays. The Milankovitch-cycles turn out to play a subordinate role for understanding the climate variabilities on the high level pursued in this study. However, there is room for other important contributions, particularly from ocean currents. At the very least, the benefit of the present analysis is to have a handy tool for estimates, particularly to quickly size risk from the CO_2-temperature relationship.

3. Interpretation

Methodologically, the present study is based on the principle that the determining forces of a certain natural phenomenon are (1) few and (2), clearly visible. The focus has been the search for the clearly visible on nature's interplay between CO_2 concentration and temperature.

With this focus, a sophisticated error calculation is regarded subordinate. Remarks on error consideration are included (Late Paleozoic) and sensitivity studies performed (Eocene relationship, Late Paleozoic). In general, the presented studies are based on long-term trends. The approach presumes that the degree of agreement between approximation and observation is clearly visible in the long-term patterns. It is perceived that a sophisticated error analysis would basically leave the degree of conclusiveness unchanged.

The major goal, uncovering reproducibility from the abundant scientific results in an 80:20 approach, is considered achieved – strongly observation-based (Eocene, Late Quaternary, Late Paleozoic), and extracting simple descriptions. The analysis recruits a single value from previous modelling: Earth's climate sensitivity for its response to the steadily increasing solar luminosity (sensitivity in the present definition as the transformation of radiation change into surface temperature change).

Due to the long time span considered in the initial derivation (15 Mio. years), the Eocene CO_2-temperature relationship reflects equilibrium climate states. Beyond conformance with measurements, the simple relationship agrees well with sophisticated simulation results (Eocene, PETM, Devonian to Triassic) offering itself as a handy tool for further analysis, and testifying reproducibility of the complex models.

The interdependency between CO_2 and Earth's climate is clearly crystallized. Either direction in the temperature relationship – CO_2 or temperature in the driver's seat – is quantified by simple means. From the presented analysis, the sceptics' argument seems difficult to be maintained that the CO_2-temperature relationship reflects a spurious correlation. At the very least with societal responsibility, the risk must be assumed that nature treats any atmospheric CO_2 concentration change according to the Eocene relationship.

Furthermore, the role of CO_2 is put into perspective with other major climate determinants, mainly those causing insolation variabilities (particularly solar luminosity and planetary albedo), with a note to the anticipated role of the ocean currents. The hope is that this will facilitate differentiation in the discussions.

Declarations

Supplementary Material: All data and code are available: Simplified climate modelling.

Conflicts of Interest: No conflict of interest is to be declared.

References

1. Wild M., Folini D., Hakuba M.Z., Schär C., Seneviratne S.I., Kato S., Rutan D., Ammann C., Wood E.F., König-Langlo G.. The energy balance over land and oceans: an assessment based on direct observations and CMIP5 climate models. *Clim Dyn* 2015, *44*, 3393–3429. https://doi.org/10.1007/s00382-014-2430-z.
2. Hansen J., Sato M., Russell G., Kharecha P. Climate sensitivity, sea level and atmospheric carbon dioxide. *Phil. Trans. R. Soc. A* 2013, 37120120294. http://doi.org/10.1098/rsta.2012.0294.
3. Hansen J., Sato M., Kharecha P., Beerling D., Berner R., Masson-Delmotte V., Pagani M., Raymo M., Royer D.L., Zachos J.C. Target Atmospheric CO_2: Where should Humanity Aim?. *The Open Atmospheric Science Journal* 2008, *2*. http://dx.doi.org/10.2174/1874282300802010217.

4. Petit J. R., Jouzel J., Raynaud D., Barkov N. I., Barnola J.-M., Basile I., Bender M., Chappellaz J., Davis M., Delaygue G., Delmotte M., Kotlyakov V. M., Legrand M., Lipenkov V. Y., Lorius C., Pépin L., Ritz C., Saltzman E., Stievenard M. Climate and Atmospheric History of the Past 420,000 Years from the Vostok Ice Core, Antarctica. *Nature* 1999, *399*, 429–436. https://doi.org/10.1038/20859.
5. Foster G.L., Royer D.L., Lunt D.J. Future climate forcing potentially without precedent in the last 420 million years. *Nat Commun* 2017, *8*, 14845. https://doi.org/10.1038/ncomms14845.
6. Scotese C. A NEW GLOBAL TEMPERATURE CURVE FOR THE PHANEROZOIC. 2016. doi:10.1130/abs/2016AM-287167. Herein: Scotese, Christopher. PhanerozoicGlobalTemperatureCurve_Small. 2016.
7. Omta A.W., Dutkiewicz S., Follows M.J. Dependence of the ocean-atmosphere partitioning of carbon on temperature and alkalinity. *Global Biogeochem. Cycles* 2011, *25*, GB1003. https://doi.org/10.1029/2010GB003839.
8. Zhu J., Poulsen C.J., Tierney J.E. Simulation of Eocene extreme warmth and high climate sensitivity through cloud feedbacks. *Sci. Adv.* 2019, *5*, eaax1874. https://doi.org/10.1126/sciadv.aax1874.
9. Soreghan G.S.; Soreghan M.J.; Heavens N.G. Explosive volcanism as a key driver of the late Paleozoic ice age. *Geology* 2019, *47*, 600–604. https://doi.org/10.1130/G46349.1.
10. Shaviv N.J., Veizer J. Celestial driver of Phanerozoic climate? *GSA Today July* 2003, *13*, *7*, 4. doi: 10.1130/1052-5173(2003)013<0004:CDOPC>2.0.CO;2.
11. Cao W., Zahirovic S., Flament N., Williams S., Golonka J., Müller R.D. Improving global paleogeography since the late Paleozoic using paleobiology. *Biogeosciences* 2017, *14*, 5425–5439. https://doi.org/10.5194/bg-14-5425-2017.
12. Han Q., Rossow W.B., Chou J., Welch R.M. Global Survey of the Relationships of Cloud Albedo and Liquid Water Path with Droplet Size Using ISCCP. *J. Climate* 1998, *11*, 1516–1528. https://doi.org/10.1175/1520-0442(1998)011<1516:GSOTRO>2.0.CO;2.
13. Keller C.B., Husson J.M., Mitchell R.N., Bottke W.F., Gernon T.M., Boehnke P., Bell E.A., Swanson-Hysell N.L., Peters S.E. Neoproterozoic glacial origin of the Great Unconformity. Proceedings of the National Academy of Sciences 2018, *116*, 201804350. DOI: 10.1073/pnas.1804350116.
14. Yang S., Galbraith E., Palter J. Coupled climate impacts of the Drake Passage and the Panama Seaway. *Clim Dyn* 2014, *43*, 37–52. https://doi.org/10.1007/s00382-013-1809-6.

Figures

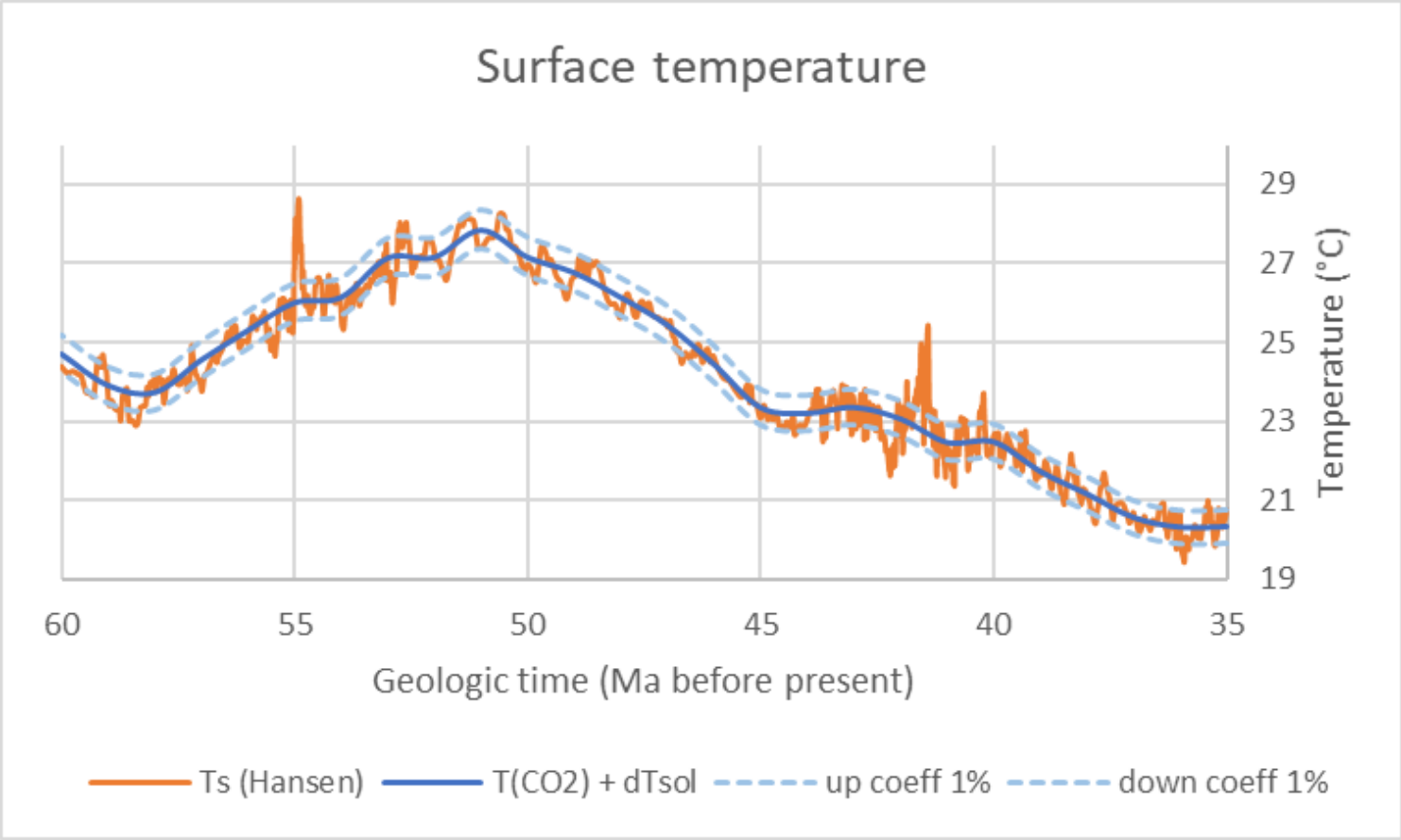

Figure 1

Mean global annual near-surface air temperature trend for the Eocene as published by [2] (wiggly orange line) and computed from the Eocene CO2-temperature relationship, T = TCO2 + ΔTsol, of the present work (smooth blue line); dotted bright-blue lines: boundaries for changes of coefficients in TCO2 by ±1 %.

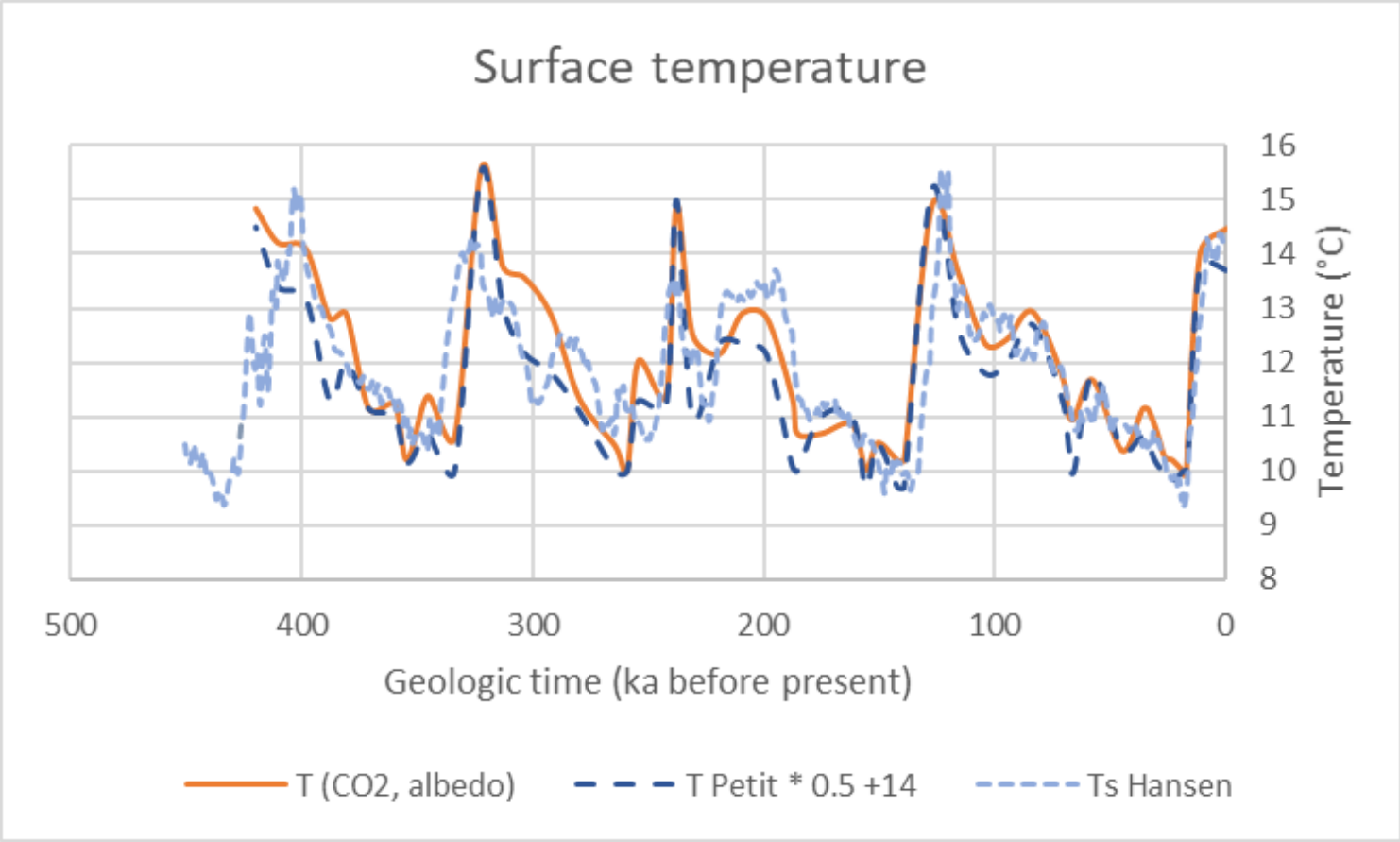

Figure 2

Surface temperatures for the Late Quaternary; 'T (CO2, albedo)': computed as T = TCO2 + ΔTice-Quaternary in the present work (orange solid line); 'T Petit' (long-dashed dark blue line): course representation of [4] as derived from the Vostok ice core proxies, multiplied by 0.5 to transform local temperature anomalies into mean global values (as in [3]), plus a 14 °C offset to translate from anomalies into absolute temperature (treated as fit parameter to match the computed temperatures, and being approximately the pre-industrial surface temperature); 'Ts (Hansen)' (short-dashed bright blue line): temperature values of [2].

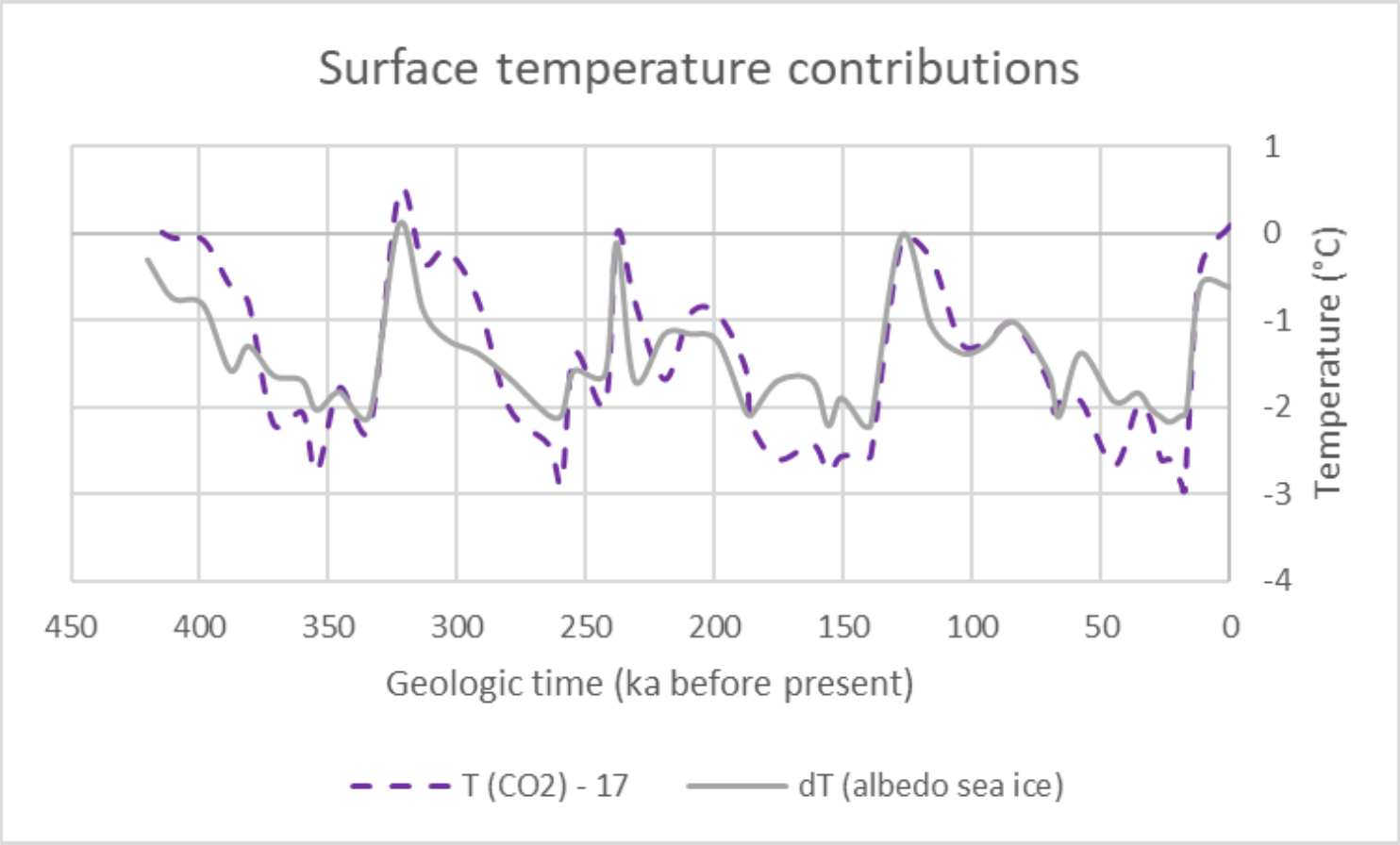

Figure 3

Surface temperature contributions to 'T(CO2, albedo)' of Figure 2; from CO2: TCO2 according to the Eocene relationship (dashed blue line, with an arbitrary offset for presentation purposes); from ice albedo: ΔTice-Quaternary (solid grey line).

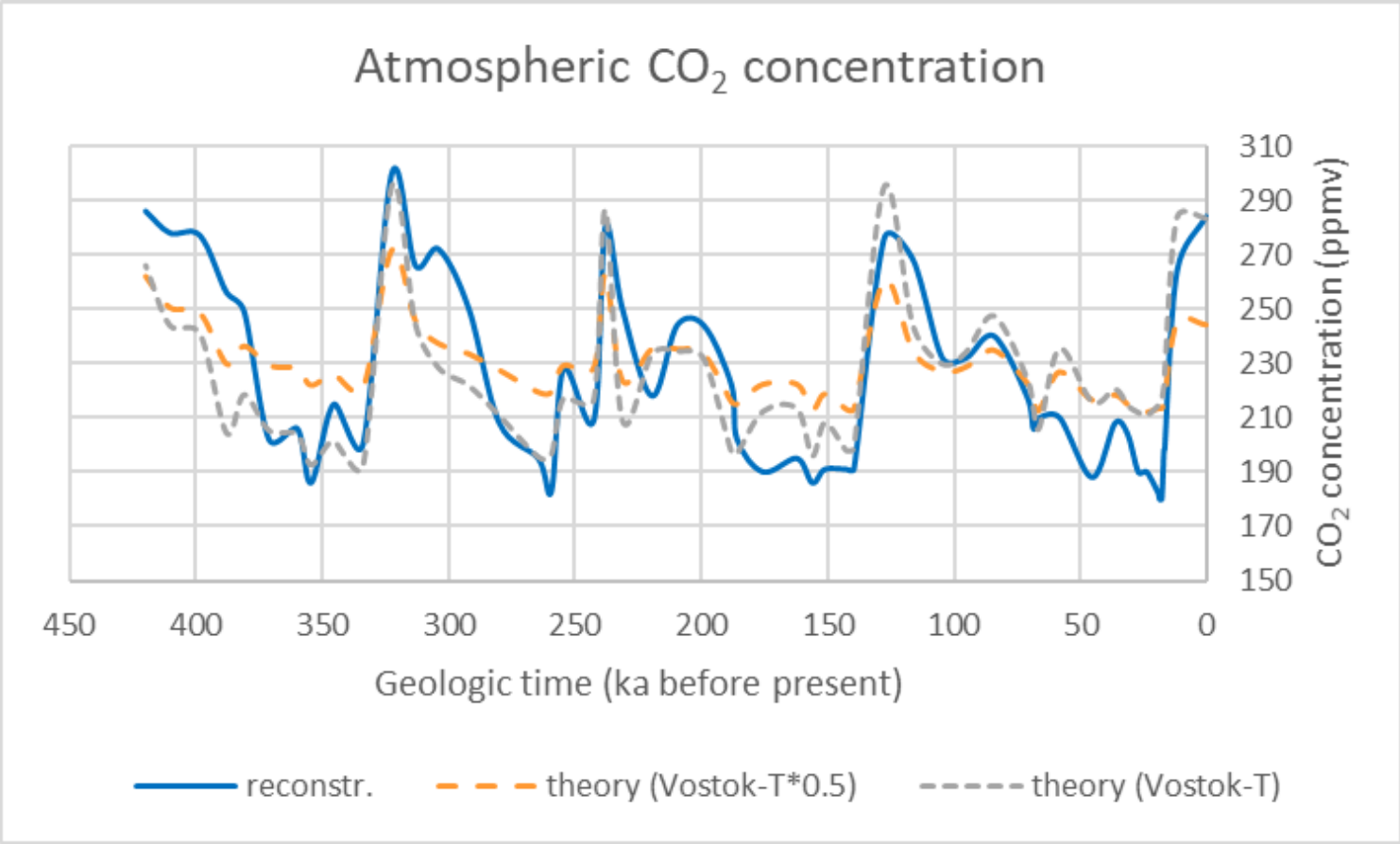

Figure 4

Atmospheric CO2 concentration in the Late Quaternary; solid blue line: course representation of proxy reconstruction [4]; dashed orange line: computed as caused by the temperature variabilities (proxy data of [4] times 0.5) according to theory [7]; dotted gray line: as before, temperature variabilities of proxy data without factor for translation from local to global mean temperature.

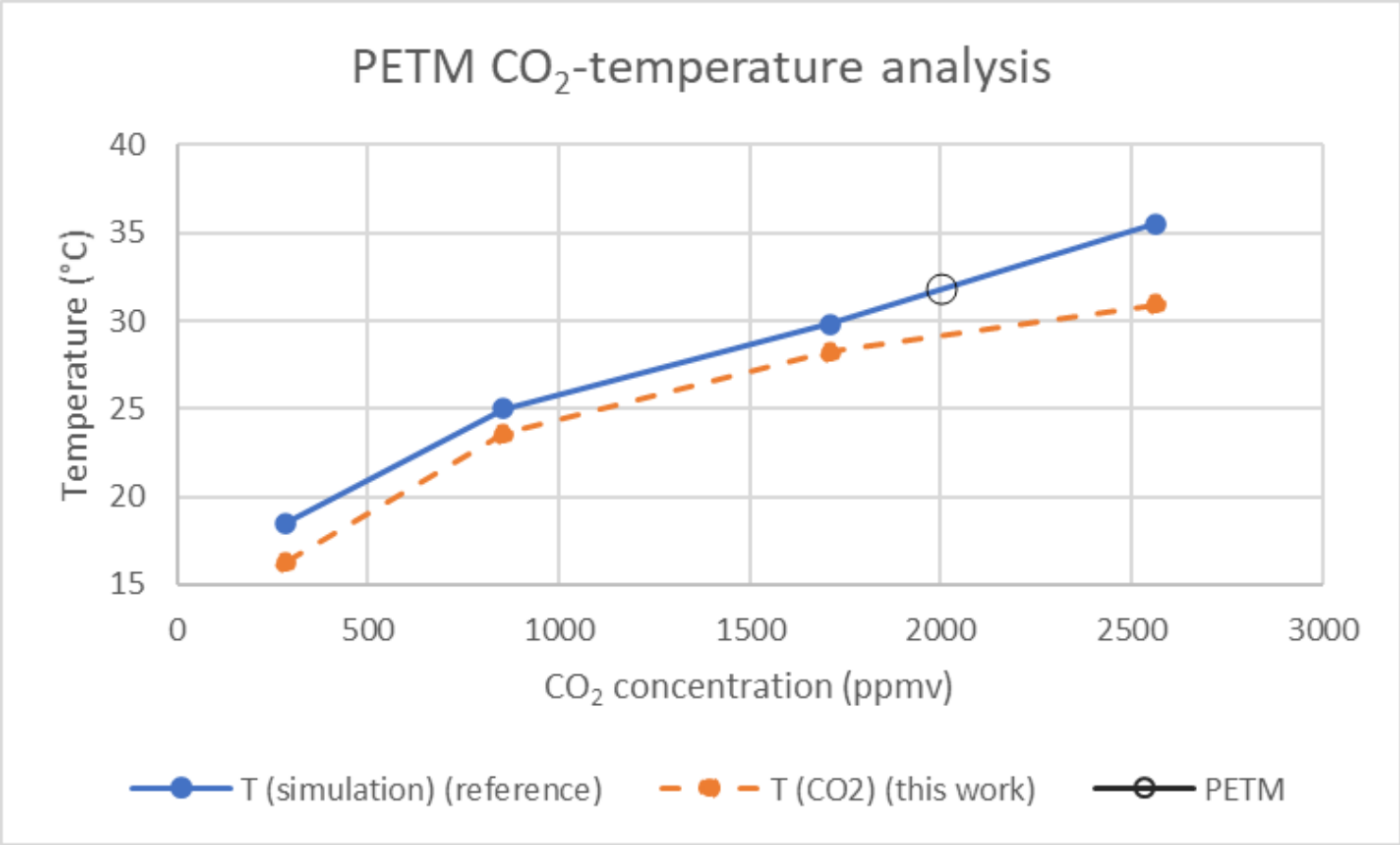

Figure 5

Surface temperature for PETM in dependence upon the atmospheric CO2 concentration, computation results as dots connected by straight lines; blue (solid connection): simulation results of [8]; black open circle: PETM condition [8]; orange (dashed connection): temperature following the CO2 concentration according to the Eocene relationship, corrected by ΔTsol for 56 Ma (this work).

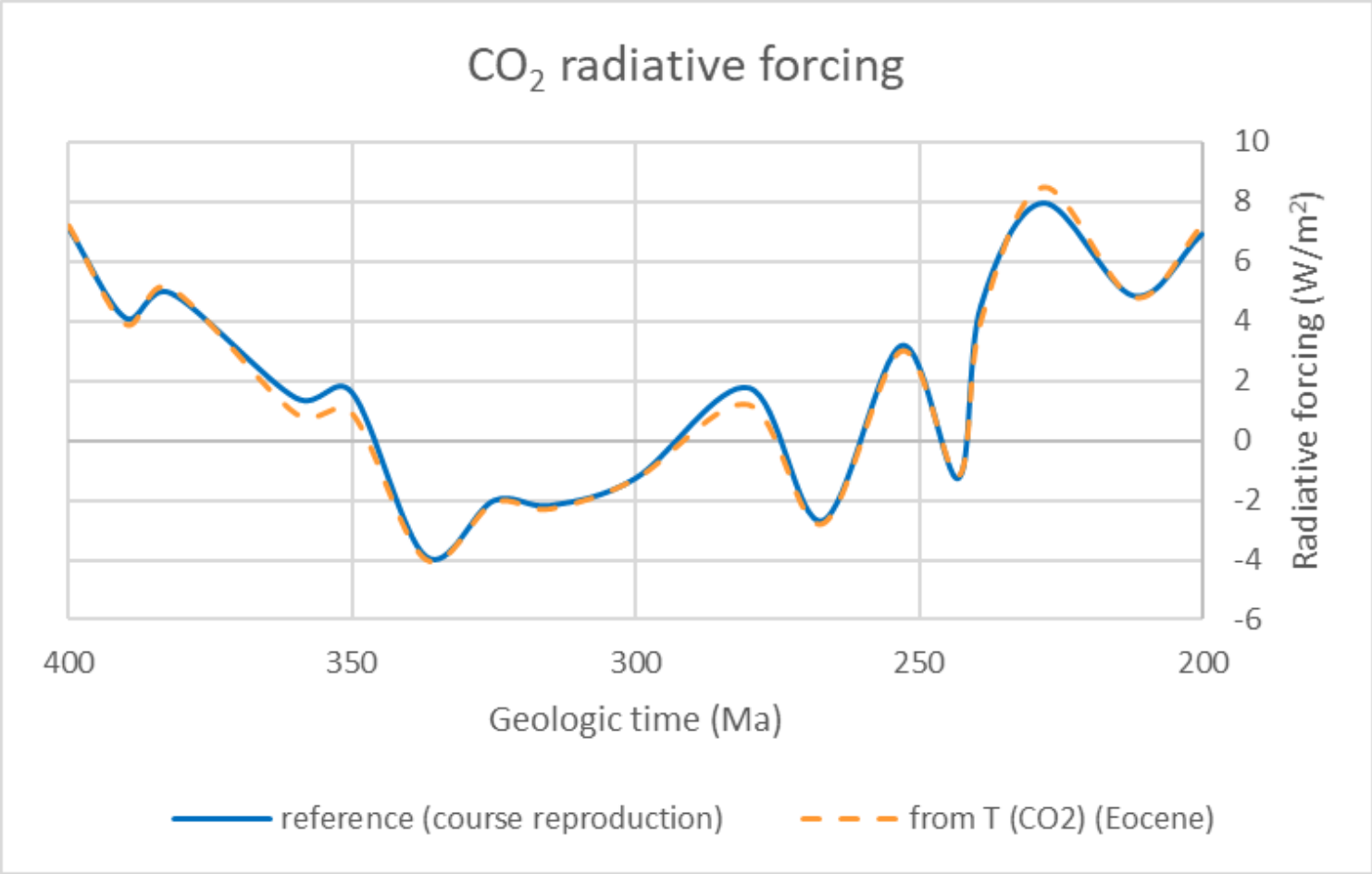

Figure 6

CO2 radiative forcing in the period 400-200 Ma BP; solid blue line: radiative forcing from [9] in course representation; dashed orange line: radiative forcing from the Eocene CO2-temperature relationship (this work) with 1.2 °C/(W/m2) as sensitivity.

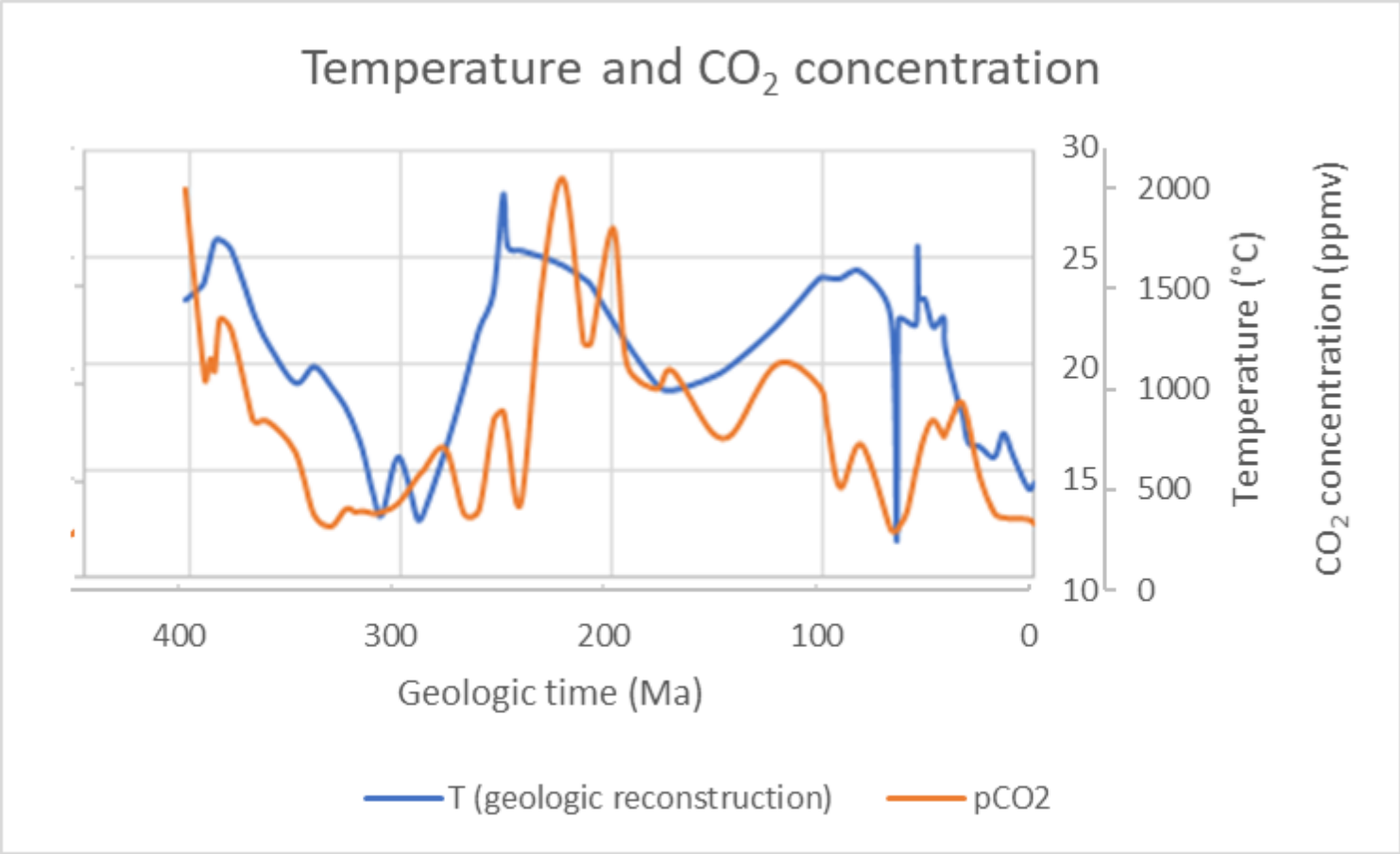

Figure 7

Reconstructed surface temperatures (course reconstruction of [6]) and CO2 concentrations [5] for the Late Paleozoic; blue (mostly upper) line: temperature, left scale; orange line: CO2 concentration, right scale.

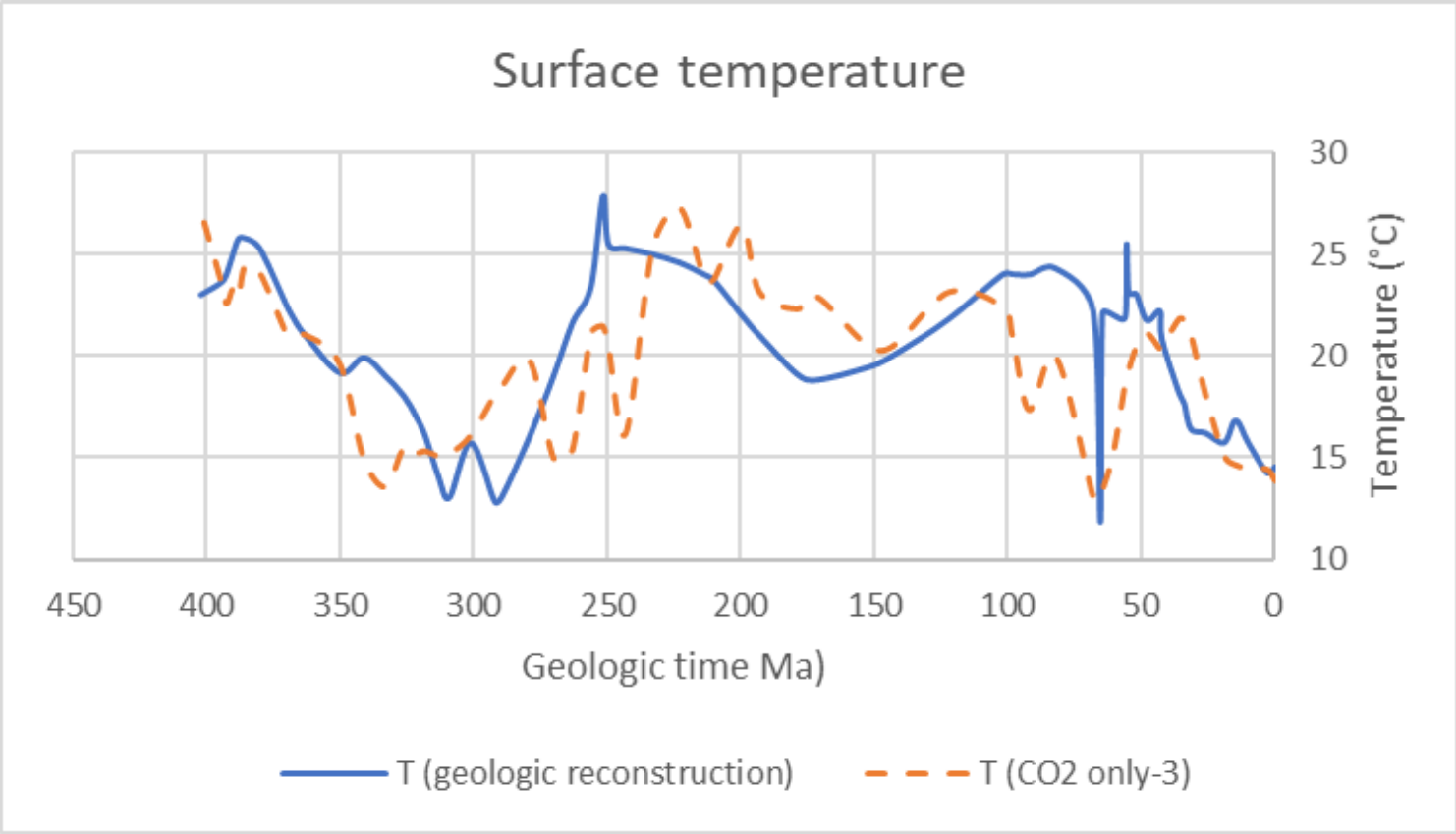

Figure 8

Surface temperatures; solid blue line: geologic reconstruction, as in Figure 7; dashed orange line: temperature determined from the CO2 concentrations [5] via the Eocene CO2-temperature relationship minus 3 °C (this work).

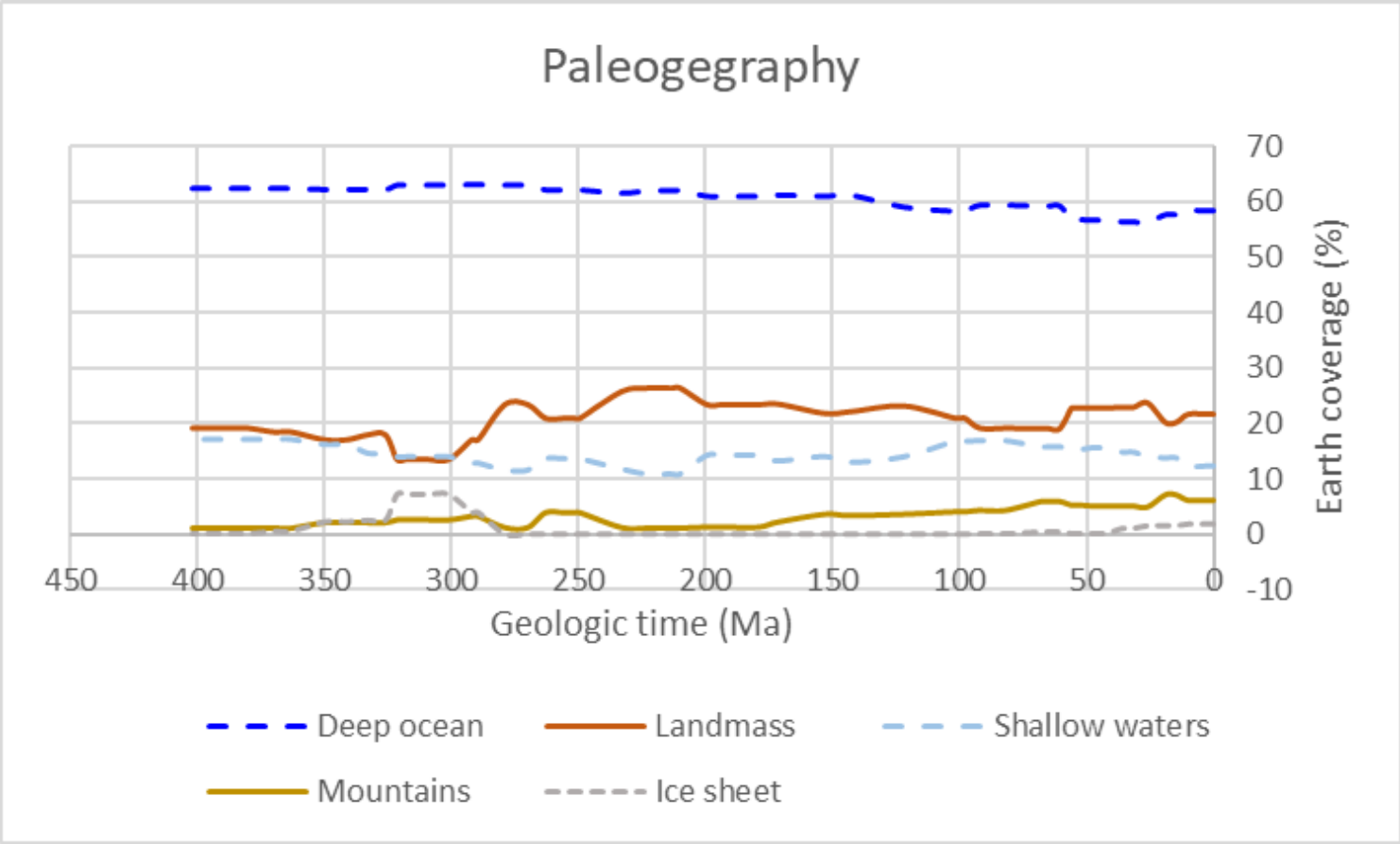

Figure 9

Paleogeographic evolvement with time; Earth coverages in % from top to bottom: deep ocean (dashed blue), landmass (solid brown), shallow waters (dashed bright blue), mountains (solid ochre), ice sheets (dotted violet).

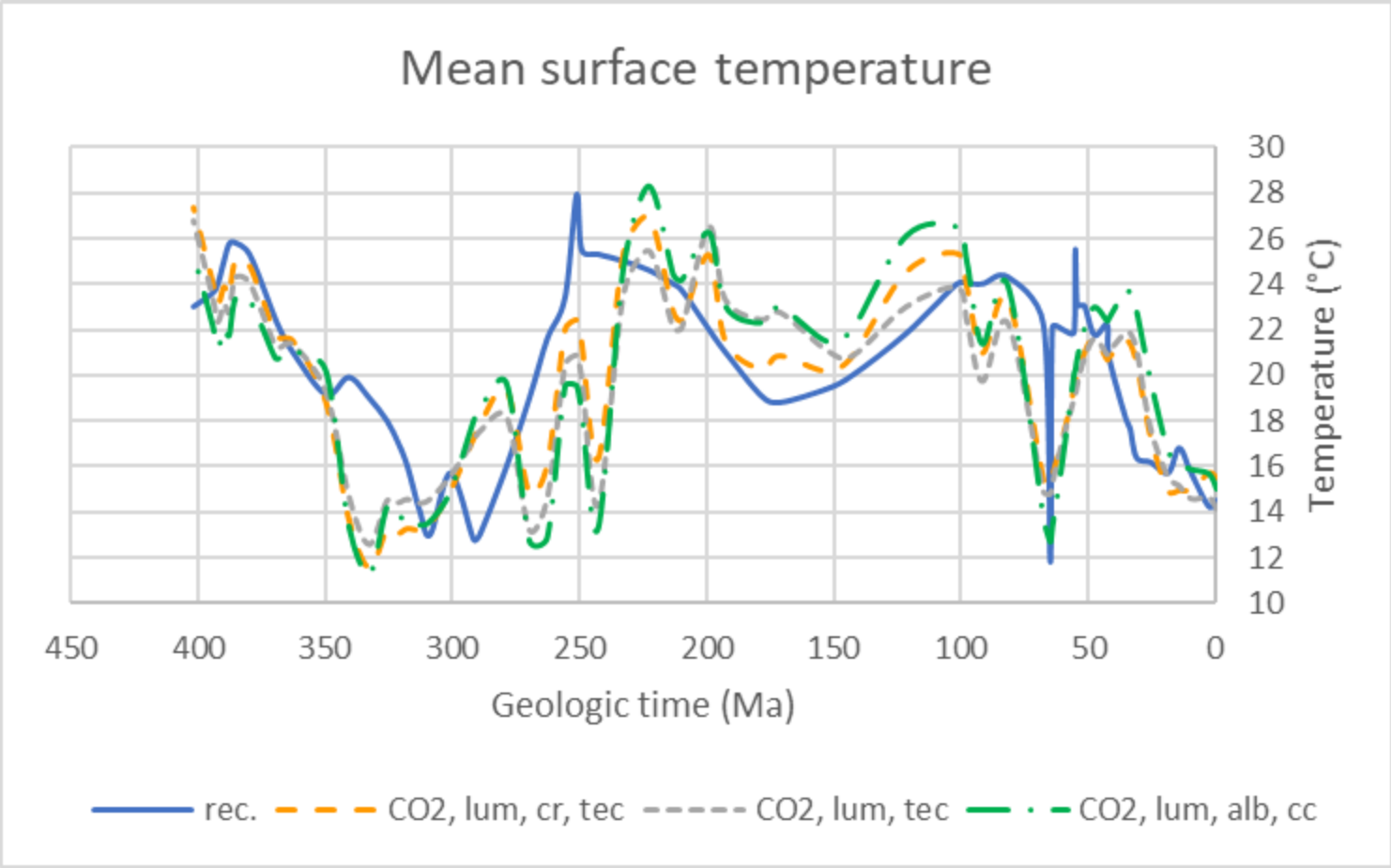

Figure 10

Surface temperatures; solid blue line: geologic reconstruction, as in Figure 7 and Figure 8; dashed orange line: determined by equation (6) of this work based on the Eocene CO2-temperature relationship; dotted gray line: as before, with cosmic ray influence switched off and ΔTtec adapted; dot-dashed green line: as before (no cosmic ray influence), with ΔTtec replaced by a snow/ice albedo approximation and continental coverage (sea level)-to-temperature proportionality (see text).

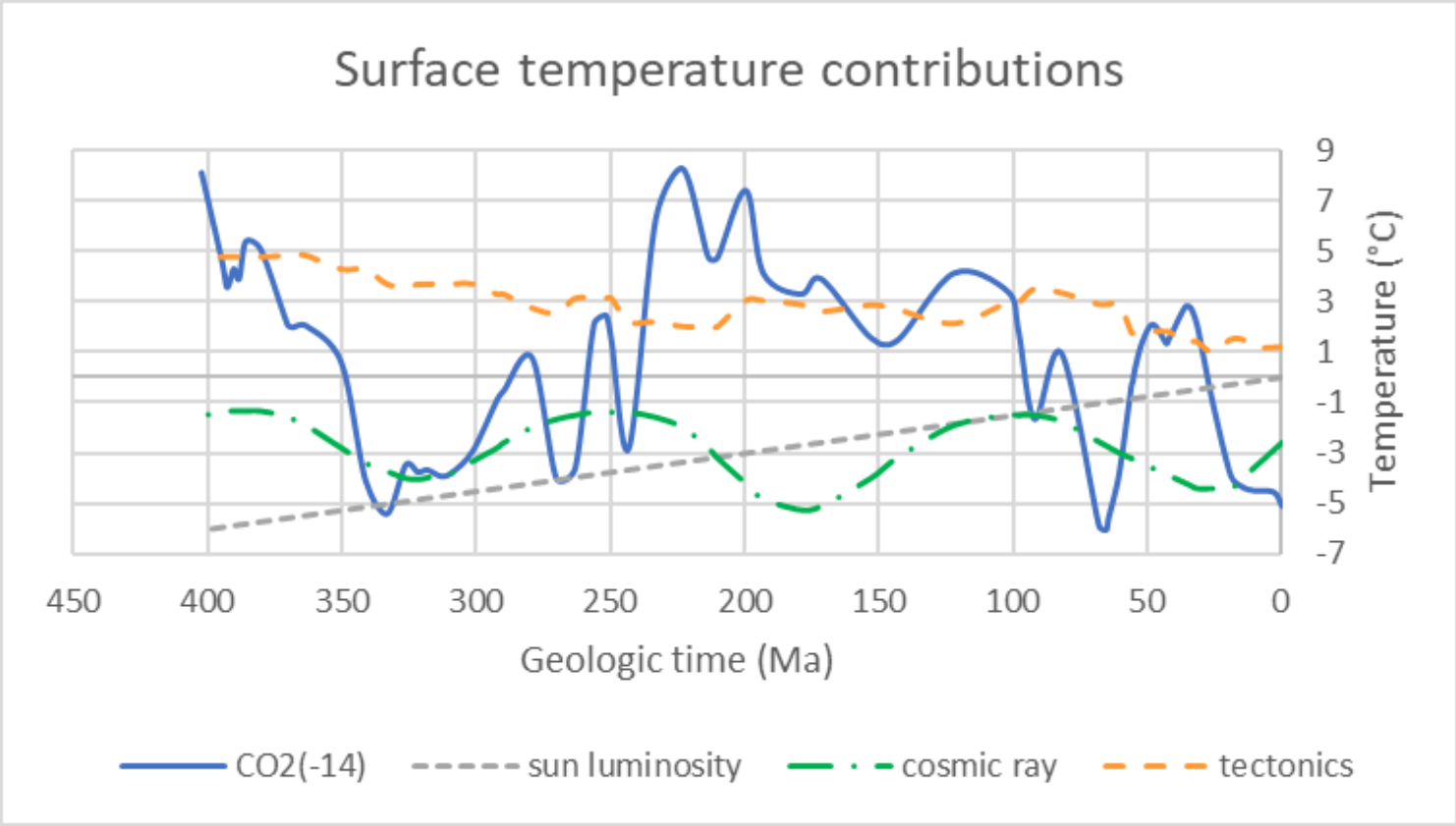

Figure 11

Surface temperature contributions to dashed orange line of Figure 10: TCO2 (solid blue) with 14 °C-subtraction for presentation purposes, ΔTsol (dotted gray), ΔTcrf (dash-dotted green), ΔTtec (dashed orange).

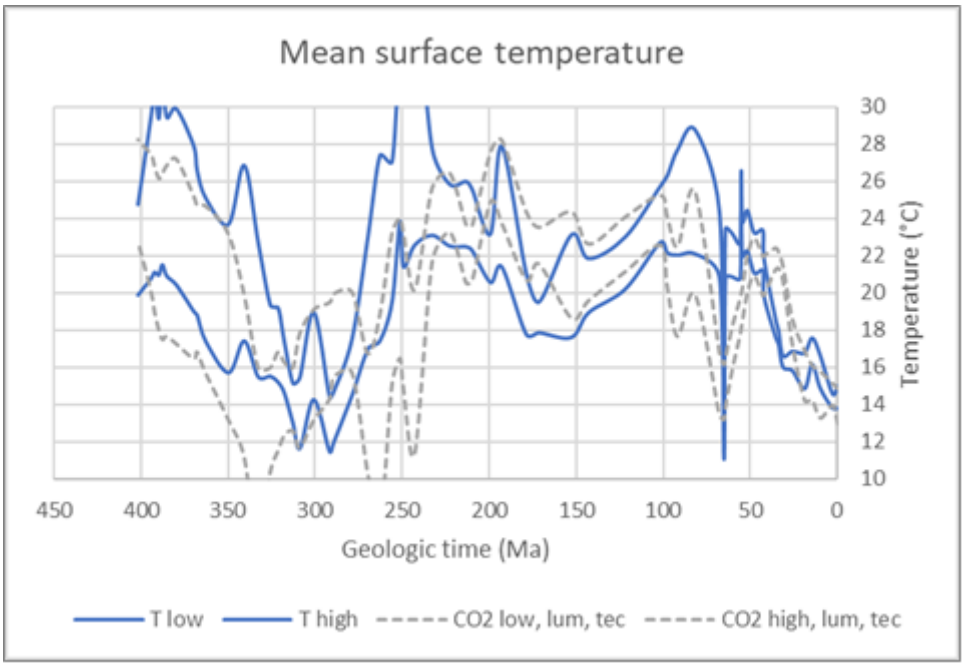

Figure 12

Uncertainty consideration for reconstructed temperature and dotted gray model of Figure 10; gray: TCO2 computed with 68%-low/high confidence envelope for pCO2 instead of maximum probability pCO2; blue: temperature envelope by emulating uncertainties from the pCO2 data via 0.3 times their relative 68%-confidence deviation from the maximum probability value.